Protein Science (2000), *9*:2294–2301. Cambridge University Press. Printed in the USA.

ACCELERATED COMMUNICATION

Design of a minimal protein oligomerization domain by a structural approach

PETER BURKHARD,[1] M. MEIER,[1] and ARIEL LUSTIG[2]

[1]M.E. Muller Institute for Structural Biology, Biozentrum, University of Basel, Klingelbergstrasse 70, CH-4056 Basel, Switzerland
[2]Department of Biophysical Chemistry, Biozentrum, University of Basel, Klingelbergstrasse 70, CH-4056 Basel, Switzerland

(Received August 15, 2000; Final Revision October 6, 2000; Accepted October 9, 2000)

Abstract

Because of the simplicity and regularity of the α-helical coiled coil relative to other structural motifs, it can be conveniently used to clarify the molecular interactions responsible for protein folding and stability. Here we describe the de novo design and characterization of a two heptad-repeat peptide stabilized by a complex network of inter- and intrahelical salt bridges. Circular dichroism spectroscopy and analytical ultracentrifugation show that this peptide is highly α-helical and 100% dimeric under physiological buffer conditions. Interestingly, the peptide was shown to switch its oligomerization state from a dimer to a trimer upon increasing ionic strength. The correctness of the rational design principles used here is supported by details of the atomic structure of the peptide deduced from X-ray crystallography. The structure of the peptide shows that it is not a molten globule but assumes a unique, native-like conformation. This de novo peptide thus represents an attractive model system for the design of a molecular recognition system.

Keywords: coiled coil; crystal twinning; ionic interactions; protein de novo design; protein folding, protein oligomerization; salt bridge

Gaining an understanding of the relationship between the amino acid sequence of a protein and its structure poses a challenging problem, primarily because proteins have such highly complex structures. However, recent progress in the de novo design of peptides has achieved significant progress in the construction of protein structures that assume a predefined fold. Harbury et al. (1998) have successfully designed a model peptide that assumes a right-handed coiled-coil conformation. Such a fold was predicted for the extremely thermostable protein tetrabrachion (Peters et al., 1996) but has only recently been proven to be a right-handed coiled coil (Stetefeld et al., 2000). Not only α-helical proteins but also β-sheet containing peptides (Kortemme et al., 1998), diiron proteins (Lombardi et al., 2000), or proteins with a specific function (Baltzer et al., 1999) have recently been designed.

Despite this considerable progress in protein design, it is still difficult to design proteins that fold into predetermined three-dimensional structures. The solution to this problem was attempted via quantifying the relative energetic contributions of short- and long-range interactions in simplified model systems such as small polypeptides (Struthers et al., 1996). These independently folded polypeptide motifs, in turn, have been successfully used as templates for construction of mini-proteins that were shown to exhibit distinct structural and functional properties (Severin et al., 1997; Baltzer et al., 1999).

The principle of short- and long-range interactions can also be found in the coiled-coil structural motif, which has been investigated in more detail, mainly by modifying the sequence of bZIP proteins (Harbury et al., 1993; Gonzalez et al., 1996; Moitra et al., 1997). Coiled coils consist of two to five amphipathic α-helices that twist around one another to form a multistranded supercoil (Lupas, 1996). Sequences of parallel left-handed coiled-coil proteins are characterized by a heptad repeat pattern of seven amino acids denoted **a** to **g** harboring mostly apolar residues in the **a** and **d** positions. The stability of the coiled coil is achieved by the systematic packing of the side chains of the amino acids in the **a** and **d** positions along a hydrophobic seam. This is called "knobs-into-holes" packing and was first postulated by Crick (1953). It has also been shown that distinct coiled-coil trigger sites within heptad-repeat-containing amino acid sequences may be necessary to mediate coiled-coil formation (Kammerer et al., 1998; Steinmetz et al., 1998). The coiled-coil trigger site of cortexillin contains a distinct pattern of inter- and intrahelical salt bridges in addition to the hydrophobic interactions occurring along the dimer interface (Burkhard et al., 2000).

The design principles for producing the shortest possible coiled-coil peptide—ideally only two heptad-repeats long—can be di-

Reprint requests to: Peter Burkhard, M.E. Müller Institute for Structural Biology, Biozentrum, University of Basel, Klingelbergstrasse 70, CH-4056 Basel, Switzerland.

vided into factors that contribute to either its monomeric α-helical stability (short-range interactions) or to its oligomeric packing (long-range interactions). The success of such a design depends on how correctly the underlying principles of coiled-coil formation and protein de novo design have been understood (see also Cohen & Parry, 1990; Munoz & Serrano, 1995). Hence, structural information is of great importance both to verify the correctness of the design and to gain insight into the atomic details of current models to correlate kinetic data with structural information. These insights can then guide the future design of de novo designed peptides with distinct structural and functional properties.

The small size of such coiled-coil peptides offers practical advantages: the newly engineered molecules can be produced efficiently and rapidly by chemical syntheses and can easily be manipulated chemically. Therefore, it is an attractive model system to study the factors responsible for protein folding and stability. Also it may be efficiently used to design a simple molecular recognition motif for applications, such as a drug targeting system (Trail & Bianchi, 1999), a protein purification and detection system (Tripet et al., 1996), and it can also be employed for the design of hybrid hydrogels (Wang et al., 1999) or biosensors (Chao et al., 1998).

Results and discussion

Factors contributing to monomeric α-helix stability

Obviously, a highly α-helical peptide would contain α-helix favoring amino acid residues, i.e., residues with a high α-helical propensity (for a review see Chakrabartty & Baldwin, 1995). In our work we have mainly focused on incorporating intrahelical salt bridges as the key stabilizing factor for monomeric α-helices (Spek et al., 1998; Burkhard et al., 2000). So far, these have mostly been classified into only two types, namely, i to $i + 3$ and i to $i + 4$ intrahelical salt bridges. Considering the geometry of an α-helix and the different lengths of the side chains of different residues, it becomes clear that an i to $i + 3$ Glu-Arg salt bridge should be energetically more favorable than an i to $i + 3$ Arg-Glu arrangement, and that an i to $i + 4$ Arg-Glu arrangement would be preferred over the i to $i + 4$ Glu-Arg salt bridge. In addition, the helix dipole would favor negatively charged side chains oriented toward the N-terminus and positively charged side chains toward the C-terminus, thus favoring positively charged residues at positions preceding the negatively charged side chains. In our design, we have preferred Arg residues over Lys residues as positively charged residues because Arg may form two charged hydrogen bonds to the carboxyl group of a Glu residue and because the guanidinium group of Arg has a decreased flexibility compared to the side chain of Lys and hence is entropically more favorable than Lys (see also Merutka & Stellwagen, 1991; Huyghues-Despointes et al., 1993). Indeed, Lys to Arg substitutions can be observed in thermophilic enzymes (Fagain, 1995) and Arg seems to be more often involved in salt bridges in coiled coils than Lys (Musafia et al., 1995; Burkhard et al., 2000).

An optimal helix capping motif was designed to compensate for the helix dipole and to generate an optimal terminal hydrogen bonding network (Doig & Baldwin, 1995; Gong et al., 1995; Lu et al., 1999). Amidation at the C-terminus and succinylation at the N-terminus of the peptides removes or even inverts the unfavorable terminal charges with regard to the helix dipole and can establish a favorable hydrogen bonding network at the N-terminus. Finally, negatively charged residues were positioned near the N-terminus while positively charged residues were placed near the C-terminus to take account of the helix dipole (Morgan & Mayo, 1998).

Factors contributing to oligomeric α-helix stability

Hydrophobic interactions occurring along the coiled-coil interface are believed to be the key driving force for the stability of the coiled coil. Stabilization of a parallel two-stranded coiled coil can be achieved, for example, with Ile in **a** positions and Leu in **d** positions (Harbury et al., 1993). While results from experimental measurements on the contribution of interhelical ionic interactions to coiled-coil stability have not been conclusive (Lavigne et al., 1996; Lumb & Kim, 1996), the recent discovery that interhelical salt bridges including charged residues even at **a** positions are a key feature of the coiled-coil trigger site of cortexillin I (Burkhard et al., 2000) point to the importance of interhelical salt bridges for coiled-coil formation and stability (Krylov et al., 1994). The helix dipole will favor negatively charged side chains oriented toward the N-terminus and positively charged side chains toward the C-terminus. Thus, the arrangement with Arg at **g** and Glu at **e′** should be energetically more favorable than the opposite arrangement. For similar reasons as discussed for the intrahelical salt bridges, Arg residues stabilize the coiled-coil structure to higher extent than Lys residues (Krylov et al., 1998).

Based on these design principles, we have de novo designed the peptide Succ-DELERR**I**RELEAR**I**K-NH_2 aimed at forming a stable parallel coiled coil with a length of only two-heptad repeats. The peptide is, in principle, able to form many intrahelical salt bridges in addition to an optimal **g-e′** Arg-Glu interhelical salt bridge (Fig. 1E).

Biophysical properties of the peptide

The oligomerization state of the peptide was determined by analytical ultracentrifugation (Table 1). In sedimentation equilibrium measurements, the peptide was found to be 93% dimeric under physiological conditions (150 mM NaCl, pH 7.0) at room temperature. Even though these results have an average error of measurement of about 20%, one can say that with higher temperatures and/or lower peptide concentration the dimer is slightly less stable. This is in agreement with the circular dichroism (CD) measurements (see below). Interestingly, when increasing the ionic strength to 2 M NaCl, the peptide switches its oligomerization state from the dimeric to the trimeric state despite the fact that its core residues were expected to favor the dimeric state (Harbury et al., 1993; Tripet et al., 2000). Such a transition between oligomerization states has not been reported before and is similar to the stabilization of a trimeric coiled coil in response to binding of a hydrophobic ligand (Gonzalez et al., 1996). Most likely this transition is due to a better shielding of the hydrophobic side chains from the very polar environment in a trimeric coiled coil compared to the situation in a dimer even though the packing of the side chains would better accommodate a dimeric structure (Harbury et al., 1993). In contrast, when replacing the Leu residues in the **d** positions of the peptide by Ile, the peptide stays dimeric under low and high ionic strength conditions (P. Burkhard, in prep.). This is again unexpected as previous experiments would predict a trimeric state (Harbury et al., 1994; Tripet et al., 2000). This clearly indicates that specific residues at specific heptad repeat positions

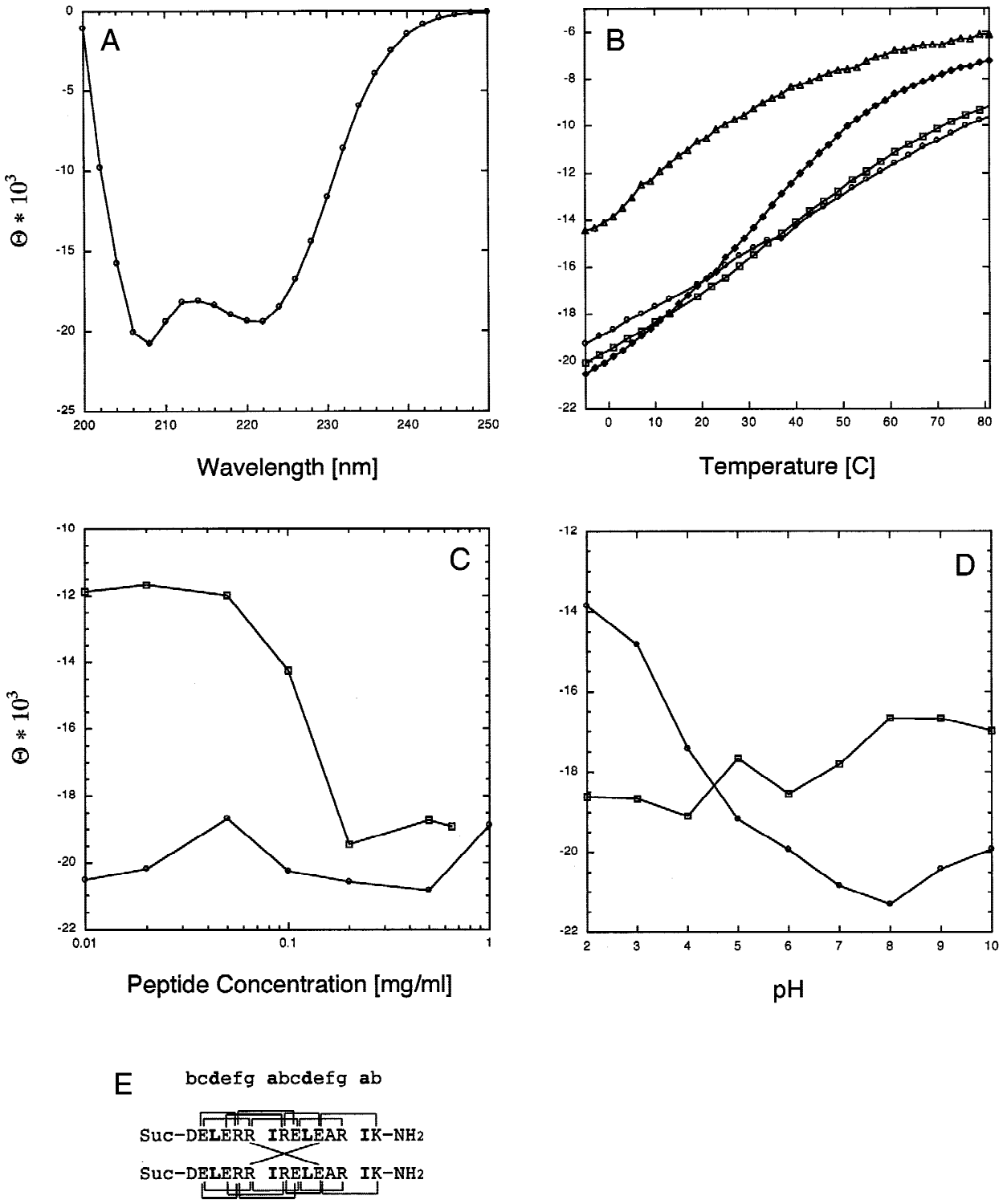

Fig. 1. CD analysis of the peptide. **A:** CD spectrum of the peptide. The peptide was analyzed in 5 mM sodium phosphate buffer (pH 7.0) and 150 mM NaCl at 0 °C. **B:** Melting curve of the peptide under different ionic strength conditions and at different pH monitored by the CD signal change at 222 nm, $[\Theta]_{222}$. The peptide concentration was always 1 mg/mL. (○) pH 7.0, 0 M NaCl; (□) pH 7.0, 0.15 M NaCl; (♦) pH 7.0, 2 M NaCl; (△) pH 2.0, 0 M NaCl. **C:** Concentration dependence of the peptide at 0 M NaCl (○) and 2 M NaCl (□) ionic strength as monitored by the CD signal change at 222 nm, $[\Theta]_{222}$. The peptide was analyzed in 10 mM Tris buffer (pH 7.0) at 0 °C. **D:** pH dependence of the peptide at 0 M NaCl (○) and 2 M NaCl (□) ionic strength as monitored by the CD signal change at 222 nm, $[\Theta]_{222}$. **E:** Sequence of the peptide with the possible intra- and interhelical saltbridges depicted as brackets and the hydrophobic core residues in bold.

Table 1. *Oligomerization state of the peptide as observed by analytical ultracentrifugation*[a]

NaCl (M)	Peptide concentration (mg/mL)	Temperature (°C)	Mw-AUC[b] (kDa)	Oligomerization state[c]
0.15	1.0	5	3.5	73% dimer[d]
0.15	1.0	20	3.9	93% dimer[d]
0.15	1.0	30	3.3	63% dimer[d]
0.15	0.3	5	3.7	83% dimer[d]
0.15	0.3	20	3.5	73% dimer[d]
0.15	0.1	20	3.3	63% dimer[d]
2.0	0.1	20	5.6	88% trimer[e]

[a]The peptide was analyzed in 10 mM Tris buffer at pH 7.0 in sodium chloride at different concentrations and temperatures.
[b]Observed molecular mass.
[c]The oligomerization state is given in percentages of dimers or trimers as calculated from the "observed" molecular mass relative to the "real" molecular mass.
[d]Assuming a monomer/dimer equilibrium.
[e]Assuming a monomer/trimer equilibrium.

cannot determine the oligomerization state per se, but that the oligomerization state is also dependent on the remainder of the sequence as well as on the buffer conditions.

According to the CD spectrum, the peptide is highly α-helical (Fig. 1A). Thermal melts of the peptide under different ionic strength conditions show a destabilizing effect of high ionic strength at higher temperature (Fig. 1B). The unfolding profile of the peptide at high ionic strength shows a higher degree of cooperativity, indicating that the unfolding of the peptide is a two-state process in which the α-helices are much more stable when they are in the coiled-coil conformation (Thompson et al., 1993). At low ionic strength, the thermal melting curve is much less cooperative and shows also at higher temperature considerable α-helicity, indicating that the monomeric α-helices themselves are very stable due to the many stabilizing intrahelical salt bridges. Also, the α-helicity of the peptide is concentration dependent at high ionic strength conditions while at low ionic strength it is not (Fig. 1C). This does not necessarily mean that the coiled coil is more stable at low ionic strength but rather that the CD signal cannot discriminate between dimers and monomers since the monomer helices are very stable at low ionic strength. This is different at high ionic strength conditions where a transition between two different states at about 0.1 mg/mL can be observed, presumably corresponding to the transition from the trimeric to the monomeric state. This corresponds to a K_d of $\sim$50 μM for coiled-coil formation.

Most remarkably, the α-helicity of the peptide is highest around neutral pH (Fig. 1B,D). This is in sharp contrast to previous observations that coiled coils containing Glu residues are more stable at low pH than at neutral pH, despite the loss of ion pairs by protonation of acidic residues at low pH (Lumb & Kim, 1995). The intrinsically higher stabilization of the coiled coil by protonated Glu has been attributed to both its higher α-helical propensity (Chakrabartty & Baldwin, 1995) and more hydrophobic character, which allows it to better pack at the dimer interface (Kohn et al., 1995). The designed peptide, however, is most stable (at low ionic strength) when its side chains are charged, indicating that the ionic interactions stabilize the α-helical conformation substantially (Fig. 1D). Furthermore, at high ionic strength and neutral pH, the coiled coil is less stable, because the contribution of the ionic interactions to coiled-coil stability is reduced due to the increased shielding of the charged side chains. This implies that the loss of stability due to shielding of the charged side chains dominates the gain of stability due to the strengthened hydrophobic interaction. This is further supported by the fact that at low pH the melting curve is nearly concentration independent (data not shown), indicating a monomolecular reaction, i.e., at low pH the peptide is mostly in its monomeric state. Hence, the ionic interactions do in fact contribute considerably to coiled-coil stability (Krylov et al., 1994; Spek et al., 1998; Burkhard et al., 2000; compare also Lavigne et al., 1996; Lumb & Kim, 1996).

Structure of the peptide

The crystal structure of the peptide at 1.2 Å resolution contains four three-stranded coiled coils in the asymmetric unit. According to the design principles employed, the peptide was found to form a parallel coiled coil (Fig. 2; Table 2). Apart from the hydrophobic packing of the core residues, the designed interhelical salt bridge of the **g-e′** type between residues Glu6 and Arg11′ appears to be the prominent and conserved feature of the structure. In all 12 possible positions within the asymmetric unit, this particular interhelical salt bridge is formed with optimal interatomic distances (Figs. 2, 3A). Moreover, the side chains of the residues involved have very low temperature factors that are comparable to those of the side chains of the core residues (Fig. 2B). This indicates that the side chains of this interhelical salt bridge are in a unique conformation. In all four trimers within the asymmetric unit, one additional interhelical salt bridge per trimer between Glu9 and Lys15′ of the type **c-b′** is formed (Fig. 3B).

Several intrahelical salt bridges according to the design principles have been found including those between Glu2 and Arg6 (Fig. 3A). None of them, however, is found in all 12 places within the asymmetric unit. The peptide was crystallized with a surprisingly low solvent content of only 25%, implying a very dense packing of the four trimers in the asymmetric unit (Fig. 4). There are many salt bridges formed between neighboring molecules within the asymmetric unit as well as to symmetry related molecules and also to bound sulfate ions. These "crystal-packing" salt bridges are in competition with the salt bridges within one trimer. The fact that none of the 12 interhelical **g-e′** salt bridges is involved in such "crystal-packing" salt bridges points again to the importance of this salt bridge for proper trimer formation. The intrahelical salt bridge arrangement, in contrast, exhibits considerable variability. As mentioned in the design principles, most of the intrahelical salt bridges are of the less favorable types for monomeric helix stabilization and may therefore more easily be involved in "crystal-packing" salt bridges.

The crystal packing as shown in Figure 4 exhibits nearly exact fourfold NCS symmetry parallel to the crystallographic *c*-axis through half of the unit cell. After half of the unit cell, the fourfold NCS axis switches its position to the center of the C-plane. This explains why this crystal form can be twinned with the twin operator (0 1 0, 1 0 0, 0 0 1). The twin fraction for this crystal as refined by the program SHELXL (Sheldrick & Schneider, 1997) was 6%. Despite the twinning of the crystal, the structure was solved by single anomalous dispersion phasing from a heavy atom derivative.

The X-ray structure also explains the high α-helix inducing potential of the N-terminal succinylation motif (Munoz & Serrano, 1995): the succinyl moiety forms as many as four hydrogen bonds

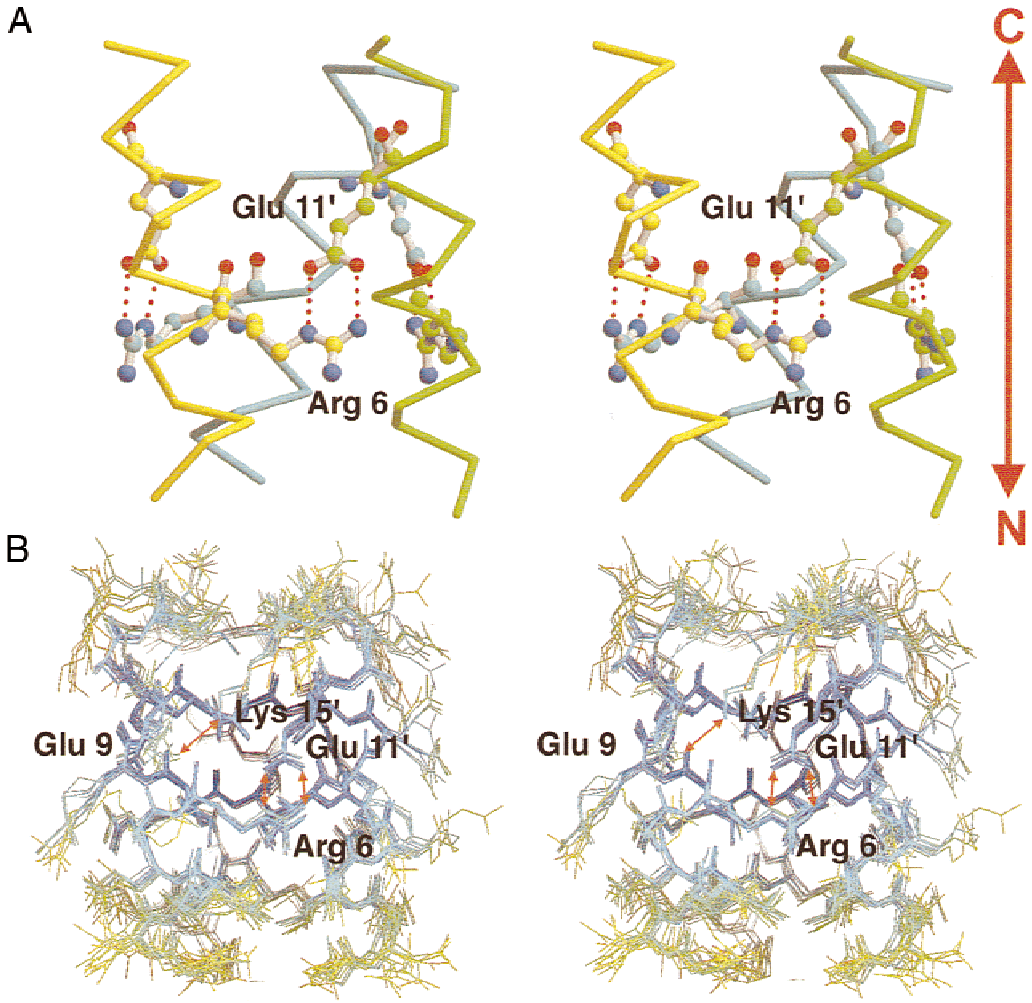

Fig. 2. Stereo view of the peptide trimer. **A:** One trimer is shown as a C_α trace with the interhelical salt bridges as red dotted lines and the residues Arg6 and Glu11 depicted as ball-and-stick model. **B:** In the same orientation, all 12 possible superpositions of the four trimers in the asymmetric unit are colored according to their atomic *B*-factors ranging from dark blue (low *B*-factors) to red (high *B*-factors). The side chains and the termini have the higher conformational variability than the peptide backbone with the exception of the side chains of Arg6 and Glu11, which form an interhelical salt bridge. Remarkably, in all 12 monomers these side chains have the same conformation and also their *B*-factors are in the same range as those of the side chains of the hydrophobic core residues. In four places, there exists also a **c-b′** interhelical salt bridge between Glu9 and Lys15′. The structures were drawn with the program O (Jones et al., 1991), MOLSCRIPT (Kraulis, 1991), and Raster3D (Merritt & Bacon, 1997).

with the N-terminal peptide nitrogens thus acting as an effective N-terminal capping box (Fig. 3C). The design of the N-terminal capping box including three negatively charged residues to compensate the positive pole of the helix dipole and a terminal succinylation that can make hydrogen bonds to the peptide nitrogen of residues 2, 3, and 4 is nicely confirmed by the X-ray structure (Fig. 3C). Even though there is considerable flexibility of the succinyl moiety, the hydrogen bonding pattern is conserved in most of 12 helices in the asymmetric unit. The C-terminus deviates from exact threefold symmetry (Fig. 3B). The three Ile14 residues all have different but well-defined side-chain conformations, and the distance between the C_α positions of the three Lys15 residues are all different. This asymmetry can be observed in all four trimers of the asymmetric unit and in all four trimers one additional interhelical salt bridge between Glu9 and Lys15′ of the type **c-b′** can be found. This salt bridge, however, is only formed between the two helices that are closest to each other. The different side-chain conformations of Ile14 allows two helices to pack closer to each other and enables the charged residues Glu9 and Lys15′ to form a salt bridge (Fig. 1B). Similarly, one could also argue that the formation of a salt bridge between Glu9 and Lys15′ forces the side chains of Ile14 to adopt a different conformation, which is only possible at the termini of the coiled coil. This would then also explain why this peptide is able to switch its oligomerization state to a trimer at high salt concentration despite the fact that the hydrophobic core residues (Ile at **a** and Leu at **d**) are thought to induce dimer formation (Harbury et al., 1993; Tripet et al., 2000).

Conclusions

In this work we have demonstrated that ionic interactions can improve coiled-coil stability considerably. In particular, the inter-

Table 2. *Data collection, phasing, and refinement statistics*

Data collection statistics	
Resolution (Å)	1.2
Observed reflections	244,675
Unique reflections	78,313
Completeness (%)	
20–2.0 Å	99.5
Overall	81.5
Phasing statistics (30.0–1.4 Å)	
R_{Cullis}[c]	0.629
Phasing power[b]	1.81
Refinement statistics (20.0–1.2 Å)	
R-factor (%)[c]	15.9
R_{free} (%)[d]	22.0
Mean *B*-factor protein atoms (Å^2)	21.51
Mean *B*-factor water atoms (Å^2)	35.99
RMSD bond distances (Å)	0.010
RMSD bond angles (°)	2.5

[a] $R_{Cullis} = \sum||F_{PH}| - |F_P + F_H||/\sum||F_{PH}| - |F_P||$.
[b] Phasing power = $[\sum|F_H|^2/\sum(|F_{PH}| - |F_P|)^2]^{1/2}$.
[c] *R*-factor = $\sum||F_{obs}| - |F_{calc}||/\sum|F_{calc}|$.
[d] $R_{free} = \geq ||F_{obs}| - |F_{calc}||/\sum|F_{calc}|$.

helical salt bridge of the **g-e′** type with an Arg residue in **g** position and Glu in **e′** position strongly stabilizes the oligomeric structure. Together with an optimal hydrophobic seam (Leu in **d** position and Ile in **a** position) and ideal helix capping boxes, we were able to design a two-heptad repeat long peptide that forms a stable parallel coiled-coil dimer under physiological conditions. Based on these findings, we are now designing short peptides able to induce specific oligomerization states as well as a hetero-dimeric coiled coil as a molecular recognition system (Chao et al., 1998). The small size of such coiled-coil peptides offers practical advantages: the newly engineered molecules can be produced efficiently and rapidly by chemical syntheses and easily manipulated chemically. Most importantly, this simple molecular recognition motif can be used eventually to design an efficient protein purification and detection system (Tripet et al., 1996) or a drug targeting system (Trail & Bianchi, 1999). Furthermore, it can also be employed in applications such as biosensors (Chao et al., 1998) or hybrid hydrogels (Wang et al., 1999).

Materials and methods

Synthetic peptides

The peptide was purchased from Neosystem (Strasbourg, France). The purity of the peptide (>95%) had been verified by qualitative amino acid and mass spectral analyses.

Analytical ultracentrifugation

AUC was performed on an Optima XL-A analytical ultracentrifuge (Beckman Instruments, Palo Alto, California) equipped with a 12 mm Epon double-sector cell in an An-60 Ti rotor. Sedimentation equilibrium runs were performed at 5 °C at rotor speeds of 48,000 and 50,000 rpm and a peptide concentration 1.0 mg/mL. Average molecular masses were evaluated by using a floating baseline computer program that adjusts the baseline absorbance to obtain the best linear fit of ln(absorbance) vs. the square of the radial distance. A partial specific volume of 0.73 mL/g was used for low ionic strength measurement and of 0.78 mL/g for the high ionic strength measurements, respectively.

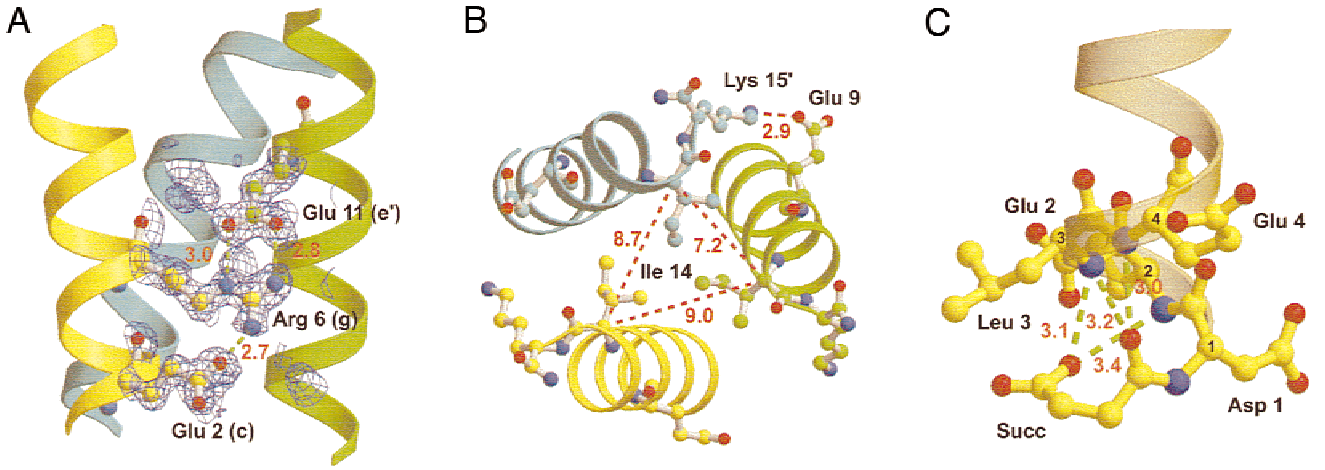

Fig. 3. Structural details of the designed peptide. **A:** A $2F_o - mF_c$ electron density of the residues involved in the highly conserved interhelical salt bridge between Arg6 **g** and Glu11 **e′** together with an *i* to *i* + 4 intrahelical salt bridge between Glu2 and Arg6. The interatomic distances (displayed as green dotted lines) are optimal to form hydrogen-bonded salt bridges. **B:** The C-terminus of the peptide is asymmetric. Between the two helices that are closest to each other (green and cyan), an interhelical salt bridge from Glu9 **c** to Lys15 **b′** is formed while between the other helices this salt bridge does not exist. All three Ile14 core residues have a different side-chain conformation. **C:** The N-terminal succinylation motif exhibits an extended hydrogen bonding network marked by green dotted lines. Despite the conformational variability found at the N-terminus, this hydrogen bonding pattern is found in all 12 N-termini of the structure thus supporting the high helix forming propensity of this N-terminal modification (Munoz & Serrano, 1995). The picture was drawn with the programs MOLSCRIPT (Kraulis, 1991) and Raster3D (Merritt & Bacon, 1997).

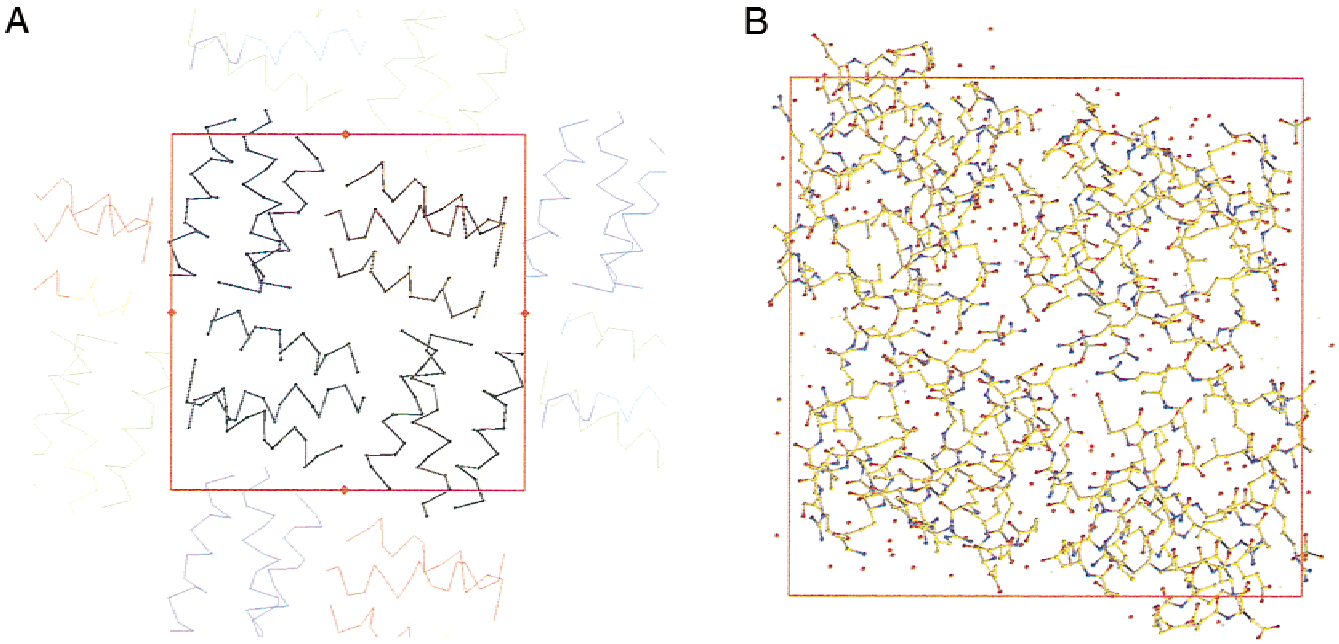

Fig. 4. Crystal packing of the peptide. **A:** The four trimers are shown as a C_α trace colored according to the residue number from red (low) to blue (high). The symmetry related molecules are drawn around the unit cell (thinner lines). The fourfold NCS axes are indicated by red squares. **B:** Only the four trimers of the asymmetric unit are shown with all atoms displayed colored according to their atom types. The picture was drawn with the program O (Jones et al., 1991).

CD spectroscopy

CD analysis of the synthetic peptide was performed on an Aviv 62 DS spectropolarimeter. Melting curves and ionic strength dependence were measured at 222 nm.

Crystallization

Crystals were grown in 24-well Limbro plates by vapor diffusion using the hanging-drop method. The 1 mL well solution contained 900 μL saturated ammonium sulfate, and 100 μL of 1 M Na-acetate buffer at pH 5.6. The 4 μL drop contained 2 μL peptide at a concentration of 60 mg/mL and 2 μL of well solution. Crystals grew within 14 days to cubes with dimensions up to $0.3 \times 0.3 \times 0.3$ mm^3. The crystals belong to the orthorhombic space group $P2_12_12_1$ with unit cell dimensions $a = 44.3$ Å, $b = 44.9$ Å, and $c = 81.0$ Å. There are four trimers in the asymmetric unit that gives a V_M of 1.65 Å^3/Da corresponding to a solvent content of only 25%.

Data collection, processing, and phasing

The X-ray diffraction data set from the trimethyl lead acetate (TLA) derivative was collected at 100 K on the X11 beamline (EMBL, DESY, Hamburg, Germany) at $\lambda = 0.91$ Å close to the absorption edge of lead ($\lambda = 0.951$ Å). This single data set was used for initial phasing based on the anomalous scattering signal as well as for subsequent refinement of the structure. Data were processed, integrated, and scaled using DENZO and SCALEPACK (Otwinowski & Minor, 1997), respectively. Initial heavy atom positions were obtained from anomalous difference Patterson maps. Heavy atom parameters were refined using the program CNS (Brünger et al., 1998). Phasing was further improved by solvent-flattening and histogram matching.

Model building and refinement

The initial atomic model was "automatically" built with the program wARP (Perrakis et al., 1997), improved using the graphics program O (Jones et al., 1991), and refined using the program SHELXL (Sheldrick & Schneider, 1997) including anisotropic *B*-factor and twinning refinement. The refined twin fraction with the twin operator (0 1 0, 1 0 0, 0 0 1) was 6%. No noncrystallographic symmetry restraints have been used during refinement. The final model comprises four trimers of the peptide, nine lead ions, four sulfate ions, and 161 water molecules. The final model has an *R*-factor of 15.9% (20.0–1.2 Å), and the free *R*-factor was calculated with 5% of the native data set aside prior to refinement and is 22.0%. Root-mean-square deviations (RMSDs) from ideality in bond lengths and angles are 0.010 Å and 2.5°, respectively (Table 2).

Accession number

Coordinates have been deposited with the Research Collaboratory for Structural Bioinformatics under the accession code 1HQJ.

Acknowledgments

We are indebted to Dr. U. Aebi for helpful discussions and all support. This work was supported by the Canton Basel-Stadt, by grants from the Swiss National Science Foundation and the Maurice E. Muller Foundation of Switzerland. SDG.

References

Baltzer L, Broo KS, Nilsson H, Nilsson J. 1999. Designed four-helix bundle catalysts—The engineering of reactive sites for hydrolysis and transesterification reactions of p-nitrophenyl esters. *Bioorg Med Chem 7*:83–91.

Brünger AT, Adams PD, Clore GM, DeLano WL, Gros P, Grosse-Kunstleve RW, Jiang JS, Kuszewski J, Nilges M, Pannu NS, et al. 1998. Crystallography & NMR system: A new software suite for macromolecular structure determination. *Acta Crystallogr D Biol Crystallogr 54*:905–921.

Burkhard P, Kammerer RA, Steinmetz MO, Bourenkov GP, Aebi U. 2000. The coiled-coil trigger site of the rod domain of cortexillin I unveils a distinct network of interhelical and intrahelical salt bridges. *Struct Fold Des 8*:223–230.

Chakrabartty A, Baldwin RL. 1995. Stability of alpha-helices. *Adv Protein Chem 46*:141–176.

Chao H, Bautista DL, Litowski J, Irvin RT, Hodges RS. 1998. Use of a heterodimeric coiled-coil system for biosensor application and affinity purification. *J Chromatogr B Biomed Sci Appl 715*:307–329.

Cohen C, Parry DA. 1990. Alpha-helical coiled coils and bundles: How to design an alpha-helical protein. *Proteins 7*:1–15.

Crick FCH. 1953. The packing of α-helices: Simple coiled coils. *Acta Crystallographica 6*:689–697.

Doig AJ, Baldwin RL. 1995. N- and C-capping preferences for all 20 amino acids in alpha-helical peptides. *Protein Sci 4*:1325–1336.

Fagain CO. 1995. Understanding and increasing protein stability. *Biochim Biophys Acta 1252*:1–14.

Gong Y, Zhou HX, Guo M, Kallenbach NR. 1995. Structural analysis of the N- and C-termini in a peptide with consensus sequence. *Protein Sci 4*:1446–1456.

Gonzalez L Jr, Plecs JJ, Alber T. 1996. An engineered allosteric switch in leucine-zipper oligomerization. *Nat Struct Biol 3*:510–515.

Harbury PB, Kim PS, Alber T. 1994. Crystal structure of an isoleucine-zipper trimer. *Nature 371*:80–83.

Harbury PB, Plecs JJ, Tidor B, Alber T, Kim PS. 1998. High-resolution protein design with backbone freedom. *Science 282*:1462–1467.

Harbury PB, Zhang T, Kim PS, Alber T. 1993. A switch between two-, three-, and four-stranded coiled coils in GCN4 leucine zipper mutants. *Science 262*:1401–1407.

Huyghues-Despointes BM, Scholtz JM, Baldwin RL. 1993. Helical peptides with three pairs of Asp-Arg and GIu-Arg residues in different orientations and spacings. *Protein Sci 2*:80–85.

Jones TA, Zou JY, Cowan SW, Kjeldgaard. 1991. Improved methods for binding protein models in electron density maps and the location of errors in these models. *Acta Crystallogr A 47*:110–119.

Kammerer RA, Schulthess T, Landwehr R, Lustig A, Engel J, Aebi U, Steinmetz MO. 1998. An autonomous folding unit mediates the assembly of two-stranded coiled coils. *Proc Natl Acad Sci USA 95*:13419–13424.

Kohn WD, Kay CM, Hodges RS. 1995. Protein destabilization by electrostatic repulsions in the twostranded alpha-helical coiled-coil/leucine zipper. *Protein Sci 4*:237–250.

Kortemme T, Ramirez-Alvarado M, Serrano L. 1998. Design of a 20-amino acid, three-stranded betasheet protein. *Science 281*:253–256.

Kraulis PJ. 1991. MOLSCRIPT: A program to produce both detailed and schematic plots of protein structures. *J Appl Crystallogr 24*:946–950.

Krylov D, Barchi J, Vinson C. 1998. Inter-helical interactions in the leucine zipper coiled coil dimer: pH and salt dependence of coupling energy between charged amino acids. *J Mol Biol 279*:959–972.

Krylov D, Mikhailenko I, Vinson C. 1994. A thermodynamic scale for leucine zipper stability and dimerization specificity: e and g interhelical interactions. *EMBO J 13*:2849–2861.

Lavigne P, Soennichsen FD, Kay CM, Hodges RS. 1996. Interhelical salt bridges, coiled-coil stability, and specificity of dimerization. *Science 271*:1136–1137.

Lombardi A, Summa CM, Geremia S, Randaccio L, Pavone V, DeGrado WF. 2000. Inaugural article: Retrostructural analysis of metalloproteins: Application to the design of a minimal model for diiron proteins. *Proc Natl Acad Sci USA 97*:6298–6305.

Lu M, Shu W, Ji H, Spek E, Wang L, Kallenbach NR. 1999. Helix capping in the GCN4 leucine zipper. *J Mol Biol 288*:743–752.

Lumb KJ, Kim PS. 1995. Measurement of interhelical electrostatic interactions in the GCN4 leucine zipper [see Comments]. *Science 268*:436–439.

Lumb KJ, Kim PS. 1996. Interhelical salt bridges, coiled-coil stability, and specificity of dimerization. *Science 271*:1137–1138.

Lupas A. 1996. Coiled coils: New structures and new functions. *Trends Biochem Sci 21*:375–382.

Merritt EA, Bacon DJ. 1997. *Raster3D: Photorealistic molecular graphics.* San Diego, California: Academic Press.

Merutka G, Stellwagen E. 1991. Effect of amino acid ion pairs on peptide helicity. *Biochemistry 30*:1591–1594.

Moitra J, Szilak L, Krylov D, Vinson C. 1997. Leucine is the most stabilizing aliphatic amino acid in the d position of a dimeric leucine zipper coiled coil. *Biochemistry 36*:12567–12573.

Morgan CS, Mayo SL. 1998. Surface design of an alpha helical protein. *Protein Sci 7*:85.

Munoz V, Serrano L. 1995. Helix design, prediction and stability. *Curr Opin Biotechnol 6*:382–386.

Musafia B, Buchner V, Arad D. 1995. Complex salt bridges in proteins: Statistical analysis of structure and function. *J Mol Biol 254*:761–770.

Otwinowski Z, Minor W. 1997. *Processing of X-ray diffraction data collected in oscillation mode.* San Diego, California: Academic Press.

Perrakis A, Sixma TK, Wilson KS, Lamzin VS. 1997. wARP: Improvement and extension of crystallographic phases by weighted averaging of multiple refined dummy atomic models. *Acta Crystallogr D Biol Crystallogr 55*: 448–455.

Peters J, Baumeister W, Lupas A. 1996. Hyperthermostable surface layer protein tetrabrachion from the archaebacterium *Staphylothermus marinus*: Evidence for the presence of a right-handed coiled coil derived from the primary structure. *J Mol Biol 257*:1031–1041.

Severin K, Lee DH, Kennan AJ, Ghadiri MR. 1997. A synthetic peptide ligase. *Nature 389*:706–709.

Sheldrick GM, Schneider TR. 1997. *SHELXL: High resolution refinement.* San Diego, California: Academic Press.

Spek EJ, Bui AH, Lu M, Kallenbach NR. 1998. Surface salt bridges stabilize the GCN4 leucine zipper. *Protein Sci 7*:2431–2437.

Steinmetz MO, Stock A, Schulthess T, Landwehr R, Lustig A, Faix J, Gerisch G, Aebi U, Kammerer RA. 1998. A distinct 14 residue site triggers coiled-coil formation in cortexillin I. *EMBO J 17*:1883–1891.

Stetefeld J, Jenny M, Schulthess T, Landwehr R, Engel J, Kammerer RA. 2000. Crystal structure of a naturally occurring parallel right-handed coiled coil tetramer [in Process Citation]. *Nat Struct Biol 7*:772–776.

Struthers MD, Cheng RP, lmperiali B. 1996. Design of a monomeric 23-residue polypeptide with defined tertiary structure. *Science 271*:342–345.

Thompson KS, Vinson CR, Freire E. 1993. Thermodynamic characterization of the structural stability of the coiled-coil region of the bZIP transcription factor GCN4. *Biochemistry 32*:5491–5496.

Trail PA, Bianchi AB. 1999. Monoclonal antibody drug conjugates in the treatment of cancer. *Curr Opin lmmunol 11*:584–588.

Tripet B, Wagschal K, Lavigne P, Mant CT, Hodges RS. 2000. Effects of side-chain characteristics on stability and oligomerization state of a de novo-designed model coiled-coil: 20 amino acid substitutions in position "d". *J Mol Biol 300*:377–402.

Tripet B, Yu L, Bautista DL, Wong WY, Irvin RT, Hodges RS. 1996. Engineering a de novo-designed coiled-coil heterodimerization domain off the rapid detection, purification and characterization of recombinantly expressed peptides and proteins [published Erratum appears in *Protein Eng*, 1997, *10(3)*:299]. *Protein Eng 9*:1029–1042.

Wang C, Stewart RJ, Kopecek J. 1999. Hybrid hydrogels assembled from synthetic polymers and coiled-coil protein domains. *Nature 397*:417–420.